Supplementary Information for

Heterostructure Nanofiber Film with Enhanced Internal Electrical Field and Surface Plasmon Resonance for Efficient Microbial Removal

Wanting Li[a], Jing Yang[b], Xin Gao[c], Yiqian Fu[a], Huiyu He[b], Pu Wang[b,d,e], Yudong Hou[c], Mankang Zhu[c],and Xiu-Hong Wang[a,d.e] *

[a]Laboratory for Biomedical Photonics, and [b] Laboratory for Advanced Laser Technology and Applications, School of Physics and Optoelectronic Engineering, Beijing University of Technology; Beijing 100124 China

[c]Key Laboratory of Advanced Functional Materials, Ministry of Education, College of Materials Science and Engineering, Beijing University of Technology; Beijing 100124, China

[d]Key Laboratory of Trans-scale Laser Manufacturing Technology, Ministry of Education, Beijing 100124 China

[e] Beijing Engineering Research Center of Laser Technology; Beijing 100124 China

*Corresponding author:

Xiu-Hong Wang, Prof.

Beijing University of Technology, 100 Pingleyuan, Chaoyang District, Beijing 100124, China

Tel: 00-86-18612921803; Email: wxh2012@bjut.edu.cn

Key words:
Ag@$BaTiO_3$/PVDF fiber film, surface plasmon resonance, piezocatalytic degradation, reactive oxygen species, anti-bacteria.

Table of contents:

1. Schematic diagram of the preparation process of PVDF composite fiber film using electrospinning

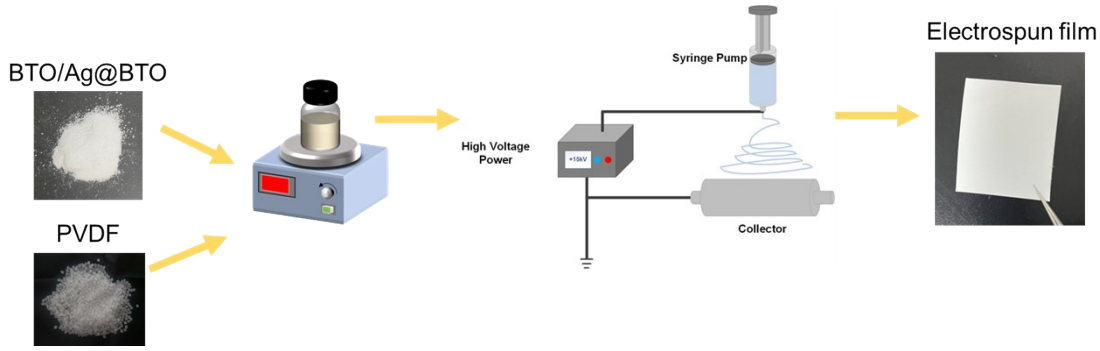

Fig. S1. PVDF powder and Ag@BTO (or BTO) nanoparticle were added to DMF solvent. The solution was stirred using a magnetic stirrer until PVDF was completely dissolved and the particles were evenly dispersed. The spinning solution was filled in a 5mL syringe with a inject rate of 0.13mm/min, the distance between the syringe and collector was 15cm and the applied voltage was 15kV. The drum rotating speed was fixed to be 1000rpm.

2. SEM images and XRD spectra of BTO prepared at different calcination temperatures

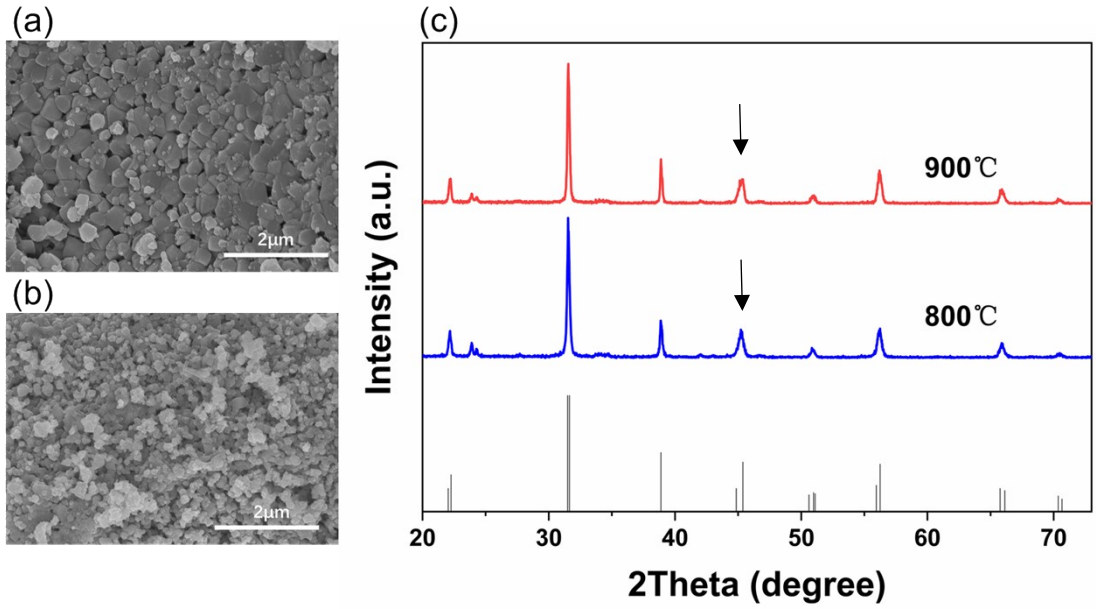

Fig. S2. SEM images of BTO prepared using sol-gel method with sintering temperature (a) 900℃ and (b) 800℃. As the calcination temperature increased, the particle size increased, and the sintering phenomenon of BTO particles also becomes apparent. (c) XRD spectral comparison of BTO prepared at different sintering temperature (900℃ 800℃). We can see that, as the temperature increased, splitting of the 2θ diffraction peak splits at 45° became apparent, indicating the presence of tetragonal phase.

3. Raman spectrum and FTIR spectrum of BTO

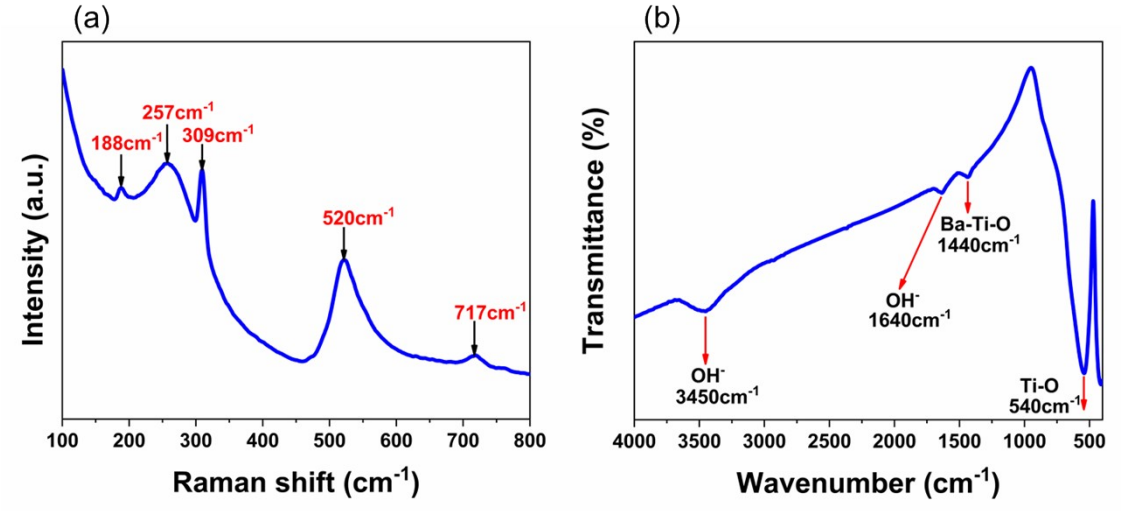

Fig. S3. (a) Raman spectrum of BTO (b) FTIR spectrum of BTO

4. TEM images of Ag@BTO

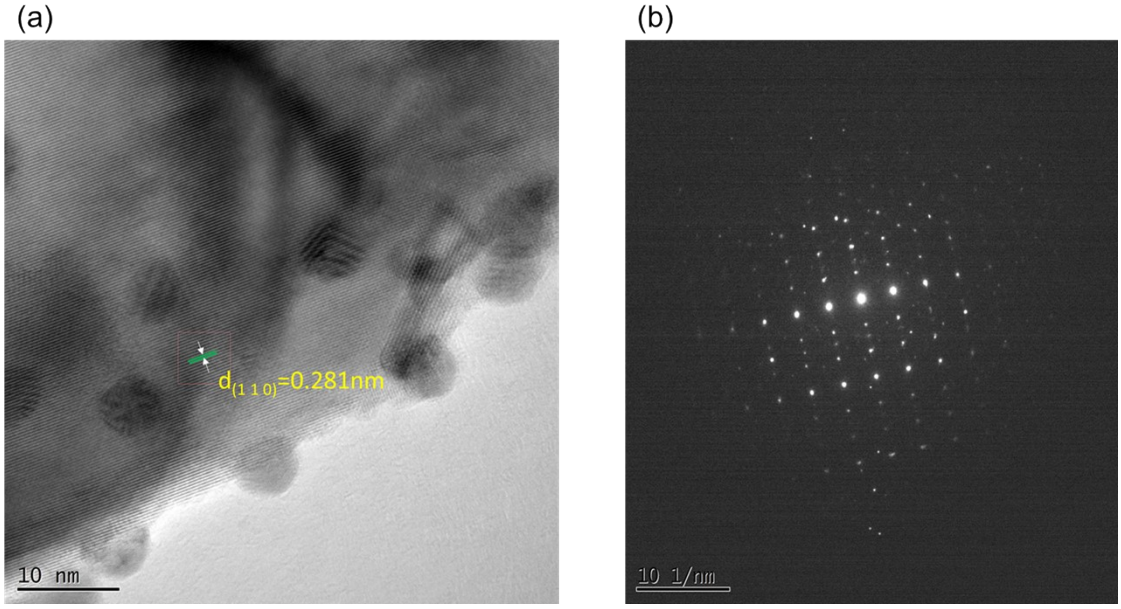

Fig. S4. (a) TEM image of Ag@BTO (b) Selected area electron diffraction pattern of BTO. This figure shows distinct lattice fringes and a clear diffraction pattern, indicating the good crystallinity of BTO particles.

5. SEM images of PVDF fiber film doped with different BTO contents

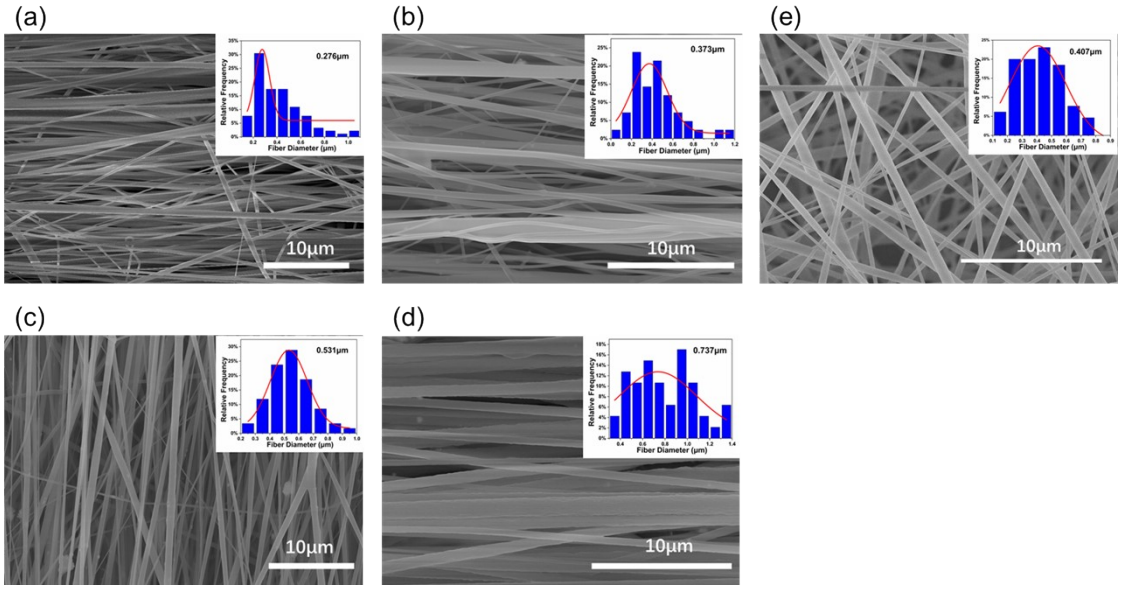

Fig. S5. SEM images of randomly selected 70 nanofibers. (a-d) SEM images of PVDF fiber film doped with 0, 2, 4, 6wt% BTO (drum rotating speed: 2800 rpm). The diameters of the fiber were shown in the table below. (e) SEM images of PVDF fiber film (drum rotating speed:140rpm). The inset figures show fiber diameter distribution of film. The diameter was measured using Image J software.

Table S1. PVDF and BTO/PVDF fibers diameter

$BaTiO_3$ mass fraction (%)	Average fiber diameter (μm)
0	0.276
2	0.373
4	0.531
6	0.737

6.Comparsion of PFM test results between PVDF fiber and Ag@BTO/PVDF fiber

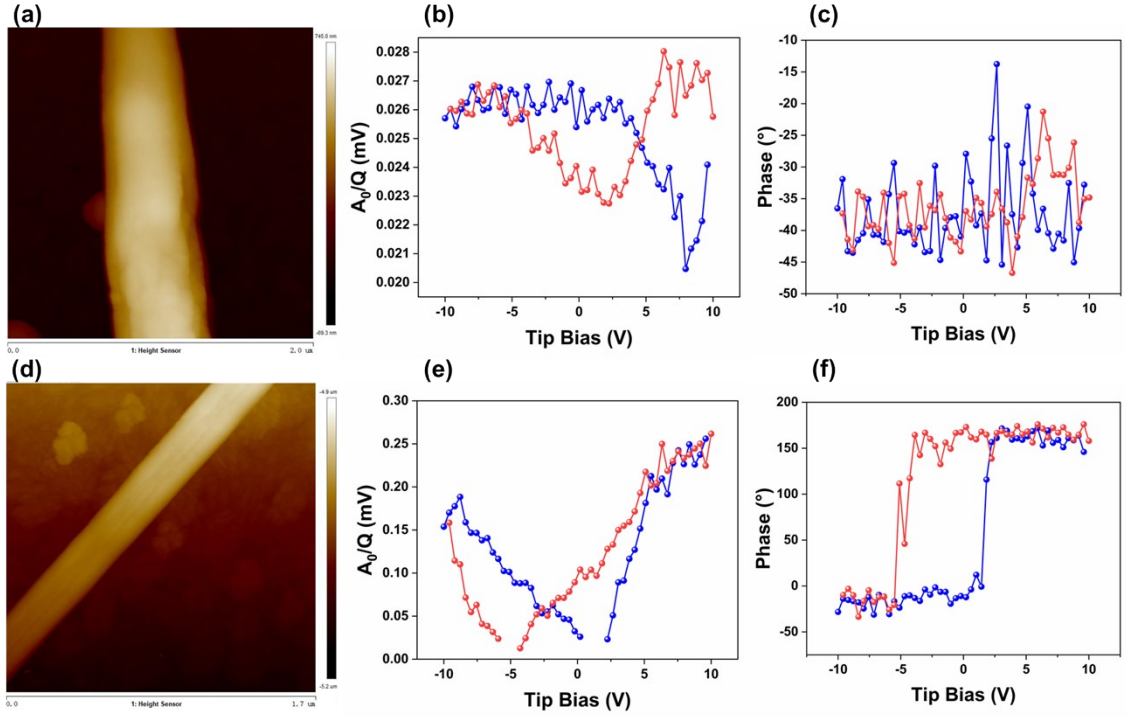

Fig. S6. PFM spectroscopy test results. (a,d) AFM images of PVDF fiber and Ag@BTO/PVDF fiber. (b,e) Amplitude (A_0/Q) of PVDF fiber and Ag@BTO/PVDF fiber. (c,f) Phase of PVDF fiber and Ag@BTO/PVDF fiber.

The PFM amplitude and phase were measured by applying the voltage from -10V to +10V by keeping the probe at a fixed point on the surface of PVDF single fiber and Ag@BTO/PVDF single fiber. Compared to the PVDF fiber, Ag@BTO/PVDF fiber shown a well defined butterfly curve and the maximum amplitude of Ag@BTO/PVDF is much greater than PVDF. Ag@BTO/PVDF had a significant 180 ° phase change hysteresis phenomenon, it indicated non-zero remant polarisation. Restricted by PFM equipment, we did not conduct HVSS-PFM experiments.

7. Comparison of output voltage of PVDF fiber film with different weight percentages of Ag@BTO nanoparticles

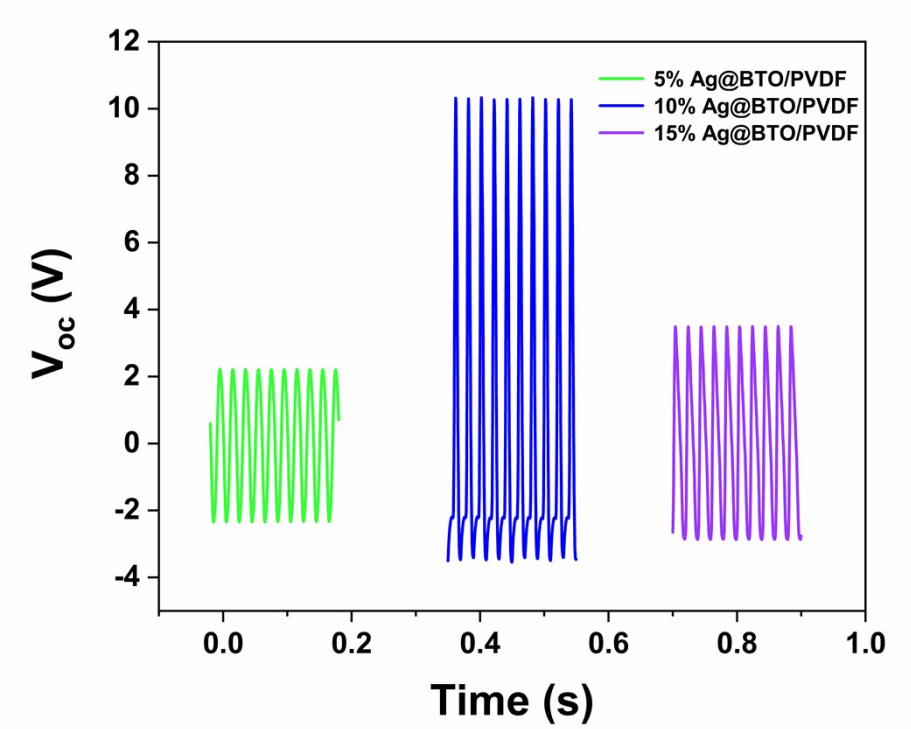

Fig. S7. Comparison of output voltage PVDF fiber film with different weight percentages of Ag@BTO nanoparticles

8. Comparison of output voltage between Ag@BTO/PVDF film and DA@Ag@BTO/PVDF film

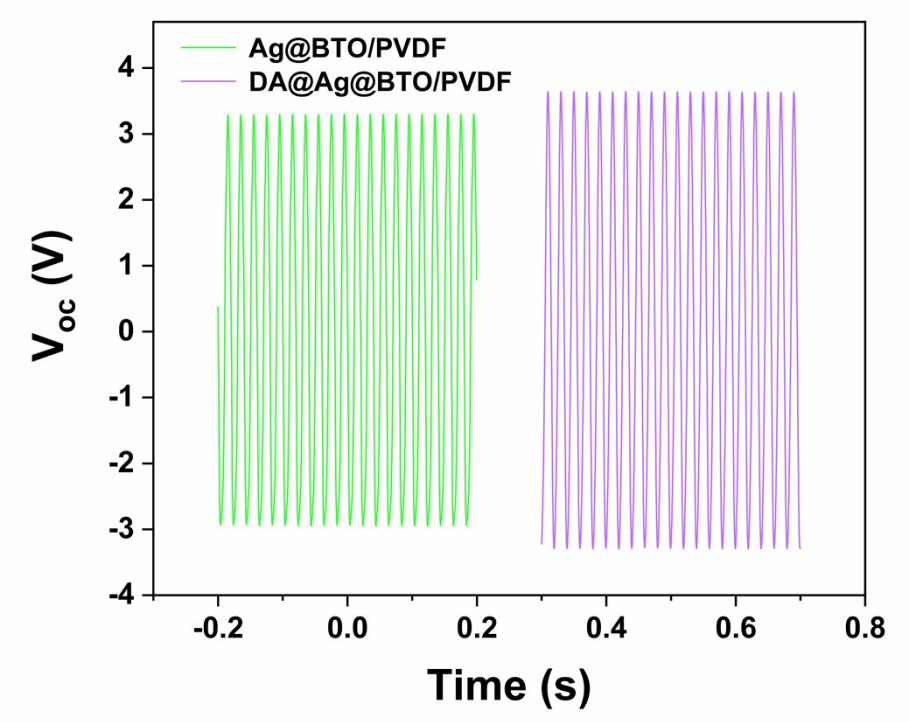

Fig. S8. Comparison of output voltage between Ag@BTO/PVDF film and DA@Ag@BTO/PVDF film.

9.Comparsion of photo-piezocatalytic degradation of MB dye between Ag@BTO/PVDF film and DA@Ag@BTO/PVDF film

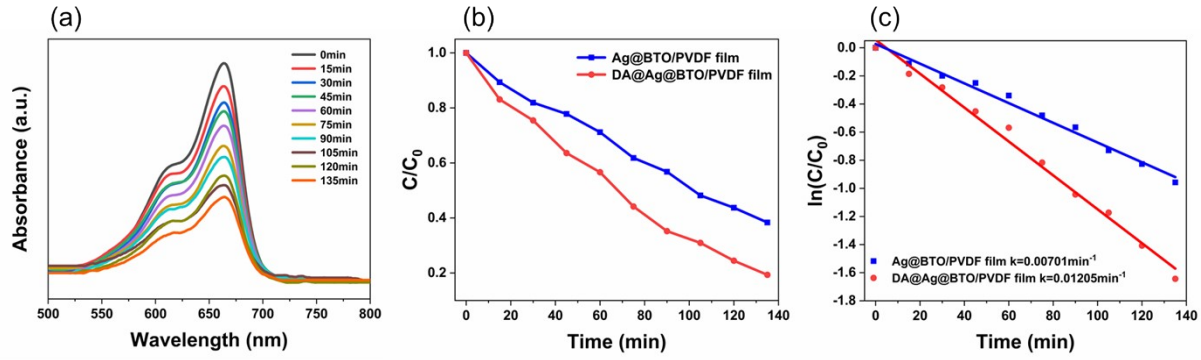

Fig. S9. (a) UV-Vis spectra of MB dye solution under photo-piezocatalysis using Ag@BTO/PVDF film after 135min (b) Comparsion of time-dependent variation of MB concentration using Ag@BTO/PVDF film and DA@Ag@BTO/PVDF film under photo-piezocatalysis treatment (c) Catalysis rate of MB degradation using Ag@BTO/PVDF film and DA@Ag@BTO/PVDF film under photo-piezocatalysis treatment.

10. Photo-piezocatalytic degradation of RhB dye

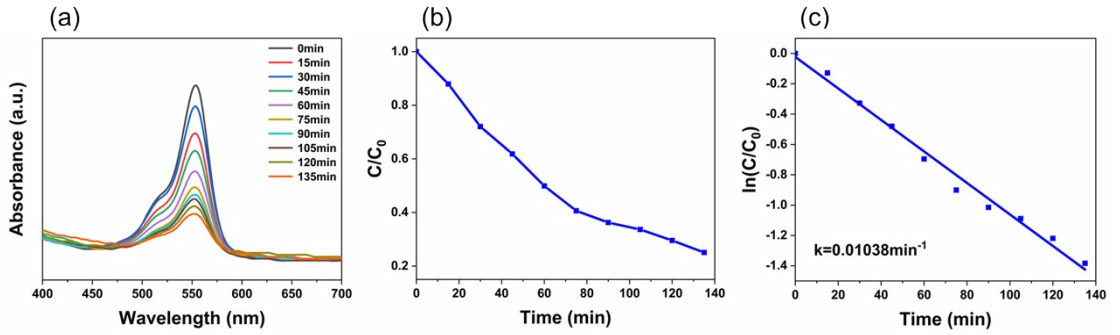

Fig. S10. (a) UV-Vis spectra of RhB dye solution undergoing photo-piezocatalysis after 135min (b) Variation in RhB concentration in solution during photo-piezocatalysis process in terms of C/C_0 with vibration time t (c) Rate of photo-piezocatalysis RhB degradation over the treatment time t

11. Antibacterial experiment of Ag@BTO/PVDF film

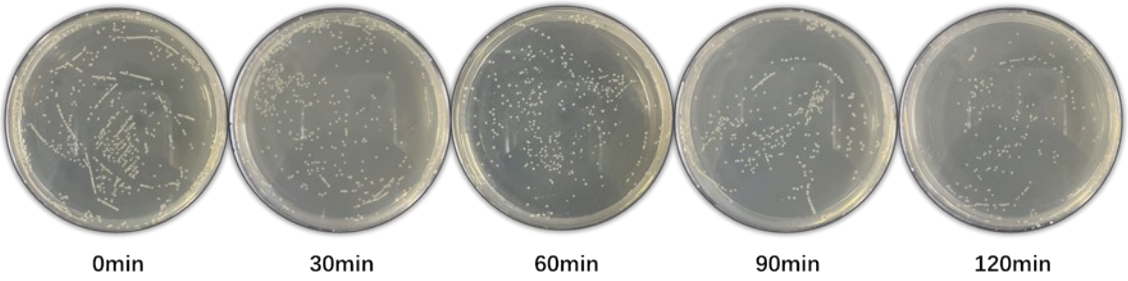

Fig. S11. Bacterial colonies of E.coli on L-B agar culture medium at various time t treated by Ag@BTO/PVDF film